Bipartite Design of a Self-Fibrillating Protein Copolymer with Nanopatterned Peptide Display Capabilities

ARTICLE *in* NANO LETTERS · OCTOBER 2010

Impact Factor: 13.59 · DOI: 10.1021/nl1024886 · Source: PubMed

NANO LETTERS

pubs.acs.org/NanoLett

Bipartite Design of a Self-Fibrillating Protein Copolymer with Nanopatterned Peptide Display Capabilities

Marc Bruning,[†,II,⊥] Laurent Kreplak,[‡,§] Sonja Leopoldseder,[†] Shirley A. Müller,[‡] Philippe Ringler,[‡] Laurence Duchesne,[II,⊥] David G. Fernig,[II,⊥] Andreas Engel,[‡] Zöhre Ucurum-Fotiadis,[†] and Olga Mayans*[,†,II,⊥]

[†]Division of Structural Biology and [‡]Maurice E. Müller Institute, Biozentrum, University of Basel, Klingelbergstrasse 70, CH-4056 Basel, Switzerland, [§]Department of Physics and Atmospheric Science, Sir James Dunn Building, Dalhousie University, Halifax, Nova Scotia B3H 3J5, Canada, and [II]School of Biological Sciences and [⊥]Liverpool Institute for Nanoscale Science Engineering and Technology, Biosciences Building, University of Liverpool, Crown Street, Liverpool L69 7ZB, U.K.

ABSTRACT The development of biomatrices for technological and biomedical applications employs self-assembled scaffolds built from short peptidic motifs. However, biopolymers composed of protein domains would offer more varied molecular frames to introduce finer and more complex functionalities in bioreactive scaffolds using bottom-up approaches. Yet, the rules governing the three-dimensional organization of protein architectures in nature are complex and poorly understood. As a result, the synthetic fabrication of ordered protein association into polymers poses major challenges to bioengineering. We have now fabricated a self-assembling protein nanofiber with predictable morphologies and amenable to bottom-up customization, where features supporting function and assembly are spatially segregated. The design was inspired by the cross-linking of titin filaments by telethonin in the muscle sarcomere. The resulting fiber is a two-protein system that has nanopatterned peptide display capabilities as shown by the recruitment of functionalized gold nanoparticles at regular intervals of ~5 nm, yielding a semiregular linear array over micrometers. This polymer promises the uncomplicated display of biologically active motifs to selectively bind and organize matter in the fine nanoscale. Further, its conceptual design has high potential for controlled plurifunctionalization.

KEYWORDS Nanofiber, protein polymer, protein engineering, self-assembly, biomaterial, peptide display system, gold nanoparticles, 1D array

Proteins are attractive building blocks for the fabrication of novel synthetic nanosystems because of their extensive functional repertoire and the convenience of their bottom-up engineering through established genetic methodologies. However, protein nanofabrication is challenged by the acute difficulty of engineering features leading to the controlled self-assembly of these intricate macromolecules. The difficulty resides in the inability to manipulate with precision and predictability the complex surfaces of these systems, which are large and rich in chemically reactive groups. Multiple studies have exploited assemblies already existent in nature that, being amenable to genetic manipulation, permit the display of exogenous biological motifs on their surface (e.g., the 60-mer E2 core from pyruvate dehydrogenase displaying GFP[1] or a 2D lattice of the bacterial S-layer protein displaying streptavidin[2]). But only a handful of studies have attempted to introduce polymerization properties in proteins through *de novo* design and bottom-up engineering.[3−5] Strategies to this effect are *domain fusion* and *formative site-directed mutagenesis*. In *domain fusion*, domains with independent association properties are concatenated into protein chimeras that self-assemble propagatively. This approach has generated a tetrahedral protein cage,[3] virus-like spherical particles,[4] and a filamentous formation.[3] However, the assemblies were polymorphic. This reflects the fact that protein surfaces are highly reactive and prone to form promiscuous interactions, particularly in crowded microenvironments. *Site-directed mutagenesis* initially uses contact information derived from the crystallographic lattices of the target proteins. The method is commonly used to stabilize pre-existent interfaces, e.g., refs 6 and 7, but it has recently been applied to the creation of new intermolecular contacts leading to better defined synthetic oligomers.[5] In brief, the engineering of ordered protein assemblies remains a formidable task.

A particular goal of biofabrication is to develop nanofibers that, by forming bioscaffolds, can emulate the eukaryotic cell matrix and, thereby, support cell- or tissue-based applications in regenerative medicine.[8,9] To date, significant success has been achieved in the production of scaffolds using self-assembling peptidic motifs,[10] commonly β-sheet rich amyloids, α-helical coiled-coils, or

* Corresponding author: telephone, +44 (0)151 7954472; fax, +44 (0)151 7954406; e-mail, Olga.Mayans@liv.ac.uk.
Received for review: 07/16/2010
Published on Web: 00/00/0000

DOI: 10.1021/nl1024886 | *Nano Lett.* **XXXX,** *xxx,* 000–000

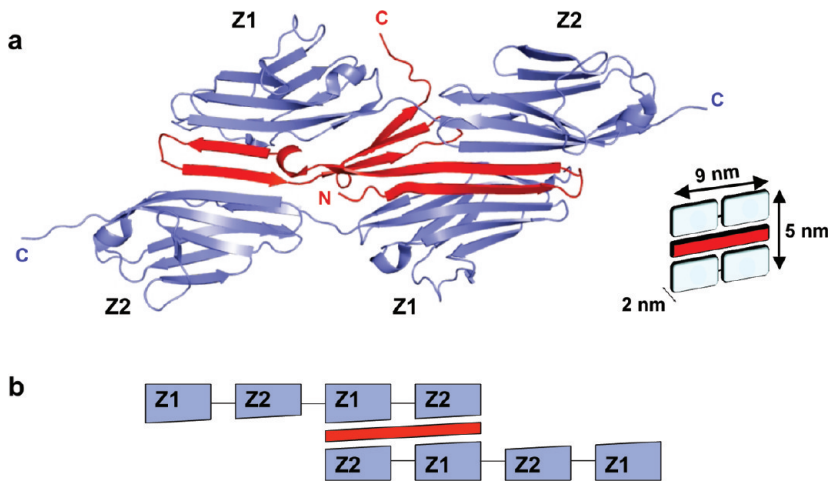

FIGURE 1. Building blocks of the self-polymerizing fibers. (a) Crystal structure of Z1Z2 from titin (blue) in complex with Tel (red) (PDB code 1YA5). (b) Design principle of self-assembling units.

collagen-like sequences. Of these, amyloidic fibers can be bottom-up functionalized via the fusion of enzymes to the amyloidic fraction, as shown using barnase, carbonic anhydrase, GST, GFP,[11] and cytochrome b_{562}.[12] However, peptidic fibers have a limited capability to support pluri-functionalization and a poorly controllable nanotopography (spatial distribution of functional groups). These properties are particularly important in scaffolds for cell growth since cells are highly responsive to both local topography[13,14] and the density of ligands on a surface.[15] Attempts to control ligand density on amyloidic fibrils have used "doping" (i.e., mixing functionalized and passive peptides).[9] But this has proven unsatisfactory because the ligand density incorporated into the fibrils was not proportional to the concentration of functional peptide in the assembly mixture and, further, peptides did not distribute evenly within the fibers resulting in clustering. An additional hurdle toward the bottom-up functionalization of peptidic systems is that the insertion of foreign sequences can hinder the assembly of the scaffold or cause unpredictable morphologies.[9,16−19] Further, functional groups displayed on the fibers can show reduced reactivity compared to their free state in solution due to poor accessibility.[11,16,17] Thus, at present, peptidic systems fall short from fulfilling the growing demand for finer and more complex functionalities in the production of bioreactive scaffolds. The use of proteins to this effect might be advantageous, since optimally designed chimeras could segregate features supporting activity and assembly and allow customization without compromising the structural scaffold. However, current synthetic protein filaments[3,20] exhibit heterogeneity and their suitability for bottom-up functionalization is unclear.

The aim of the present study is to develop a biocompatible, reactive scaffold, where functionality is easily modifiable through peptidic display. To this end, we have explored a new design avenue toward the rational fabrication of protein fibrils with controlled self-association properties and amenable to bottom-up customization. Our strategy couples domain fusion with secondary complementation, where the fused domains do not self-associate but their interaction is induced by a second protein that acts as specific cross-linker. The resulting fibers are copolymers with a homogeneous and predictable morphology and with decoupled assembly and functional regions. For this, we have exploited the associative properties of the titin muscle filament and telethonin (Tel), a small protein that cross-links the two N-terminal Ig domains of titin, Z1Z2, in the sarcomere. Tel "sandwiches" itself between two antiparallel Z1Z2 doublets, forming an intermolecular β-sheet that spans the three components[21] (Figure 1a). The binding is robust and highly specific within the crowded in vivo environment of the sarcomere. By producing a Z1Z2−Z1Z2 fusion tandem (hereby Z_{1212}), containing two binding sites for Tel and able to undergo cross-linking in an abutting fashion (Figure 1b), a noncovalent nanofibril was engineered. Structural data for the Z1Z2/Tel complex[21] and the isolated Z1Z2[22,23] suggested the sequence **VQ**GETT**QA** as suitable linker, where **VQ**GET is the C-terminus of Z2 and TT**QA** the N-terminus of the subsequent Z1 (residues in bold are integral to the flanking Ig folds). Computer modeling predicted that linker residues TT are free from interactions and, thus, can act as a mechanical hinge allowing intermodular motions.

The Z_{1212} tandem and a minimal Tel variant (reduced to its titin-interacting region)[22] were genetically engineered, expressed recombinantly in bacteria, and purified to homogeneity by chromatography (supplementary section S1 in the Supporting Information). The monomeric state of the Z_{1212} chimera was confirmed by SEC-MALS (supplementary section S2 in the Supporting Information), suggesting its suitability to form monofibers with a low tendency to bundle. Z_{1212} and Tel were assembled by mixing in an aqueous solution (supplementary section S1 in the Support-

DOI: 10.1021/nl1024886 | *Nano Lett.* **XXXX,** *xxx,* 000–000

ing Information). Electrophoresis confirmed the capability of the fusion tandem to bind Tel and the presence of high M_r species in the solution mixture (supplementary Figure S1b,c in the Supporting Information). Imaging of negatively stained assembly samples (supplementary section S3 in the Supporting Information) by transmission electron microscopy (TEM) revealed nanofibers several micrometers in length (typically 5−10 μm), demonstrating the productive interaction of building blocks on a large scale and the success of the design concept. Two fiber types were identified: (i) semirigid tapelike fibers with a diameter of 13.4 ± 1.6 nm (n = 100) (Figure 2a); and (ii) highly flexible, thin, curly fibers with a diameter of 7 ± 1.6 nm (n = 100) (Figure 2b). The tapelike fibers (i) were blunt-ended with apparent helicity and stiffness. The curly fibers (ii) had abundant kinks and bends, leading to strong coiling. The spacing between successive kinks was as small as 9−10 nm. This value agrees well with the length of the Z1Z2/Tel structural unit and suggests that the chain bends where the free, single-stranded linkers connect each unit along the fiber. Neither of the fiber types showed a detectable tendency to bundle. TEM imaging of assembly mixtures revealed that tapelike (i) and curly (ii) fibers occurred together in solution, forming networks (Figure 2c−g).

The observed fiber types closely resembled assembly models predicted in silico (supplementary section S4 in the Supporting Information). Simulations suggested that the design principle supports two main modes of assembly: (a) a longitudinal mode where Z_{1212}/Tel are parallel to the direction of fiber growth; and (b) a stacking of blocks perpendicular to the fiber axis. Models constructed according to a longitudinal assembly closely reproduced the features of curly fibers (ii) (Figure 2b). This association mode was permissive to virtually any Z_{1212} tandem conformation that the algorithm selected randomly from a family of conformers for incorporation into the growing fibril. The calculated model fibers exhibited high flexibility arising from the conformational dynamics of the engineered linker, which formed single chain points tethering Z1Z2/Tel units along the polymer. Similarly, models constructed according to a transversal association of components closely reproduced the characteristics of the tapelike fibers (i) (Figure 2a) (model supported by experimental scanning transmission electron microscopy (STEM) data; supplementary section S3 in the Supporting Information). In this fiber type, the conformation of Z_{1212} tandems appeared to be restrained by stacking interactions that result in a more regular, long-range organization of the fiber. Although the simulation models are only qualitative and do not exclude other possible modes of interaction, they closely reproduce experimental results and demonstrate the feasibility of both fibrillation processes.

The Z_{1212}/Tel system has a high potential for functionalization as foreign peptidic sequences can be introduced at points spatially remote from the assembly interface, e.g., the N- and C-termini of Tel (that protrude loosely from the fibril axis) or the exposed loops in the Z1 and Z2 domains. In this work, we explored the capability of Tel to act as a display module. We introduced a specific N-terminal His_6-tag recognition motif able to bind gold nanoparticles (AuNP) functionalized with TrisNiNTA groups. To avoid fibril cross-linking, the AuNP employed had only 1.5 TrisNiNTA groups per particle on average.[24] TEM imaging showed that tagged Tel successfully recruited the functionalized AuNPs to the fiber (Figure 3). The AuNPs, with a diameter of 6.55 ± 0.95 nm (n = 100), were evenly distributed along the fiber with an average edge-to-edge inter-NP distance of 5.04 ± 2.09 nm (n = 100). The periodic array formed is markedly finer and more regular than those previously reported for peptidic polymers[9,25,26] (e.g., amyloidic fibrils decorated with streptaviding achieved periodicity at ca. 50 nm with a distance distribution of 25−200 nm[25]). In brief, the binding motifs at this display point did not compromise scaffold assembly, were accessible and functional within the fiber, and resulted in a fine periodical functionalization of the scaffold yielding a semiregular linear array.

In conclusion, engineering from first principles morphologically homogeneous protein nanofilaments (undergoing infinite assembly in one dimension but with suppressed heterogeneous association) is challenging. The features of the protein fibers engineered here closely match those predicted through simulation, and the Z_{1212}/Tel components are robust and relatively inexpensive to produce recombinantly. The polymer design follows a bipartite principle that segregates customizable features supporting function (loops and terminal tails) and regions mediating assembly, promising the uncomplicated bottom-up display of biologically active motifs, as demonstrated by the specific attachment of AuNP to the tagged Tel subunits. The functional retailoring of the fibers can be easily performed through standard genetic engineering by replacement of the His-tag motif in Tel by other desired biomotifs (e.g., cell attachment sites, signaling modules, or peptidomimics to support cell-based applications). Further, the display of functional groups in these fibers is regularly spaced in the nanoscale. Predictably, the system also offers enhanced potential for the nanotopographic sculpting of multifunction, where active elements can be introduced simultaneously at several display positions (e.g., both the N- and C-termini of Tel). This would ensure the stoichiometric presence of functions in the fiber and their vicinal arrangement to support, e.g., orthogonal recognition, the coupling of reporter and capture probes or complementary catalytic activities by fusion of enzymatic modules. We also demonstrate that the fibers can interface with nonbiogenic materials, like AuNPs, in an orderly manner. AuNPs are powerful molecular detection probes that can be easily multifunctionalized to carry a controlled number of biofunctions, such as cell or protein

DOI: 10.1021/nl1024886 | *Nano Lett.* **XXXX,** *xxx,* 000−000

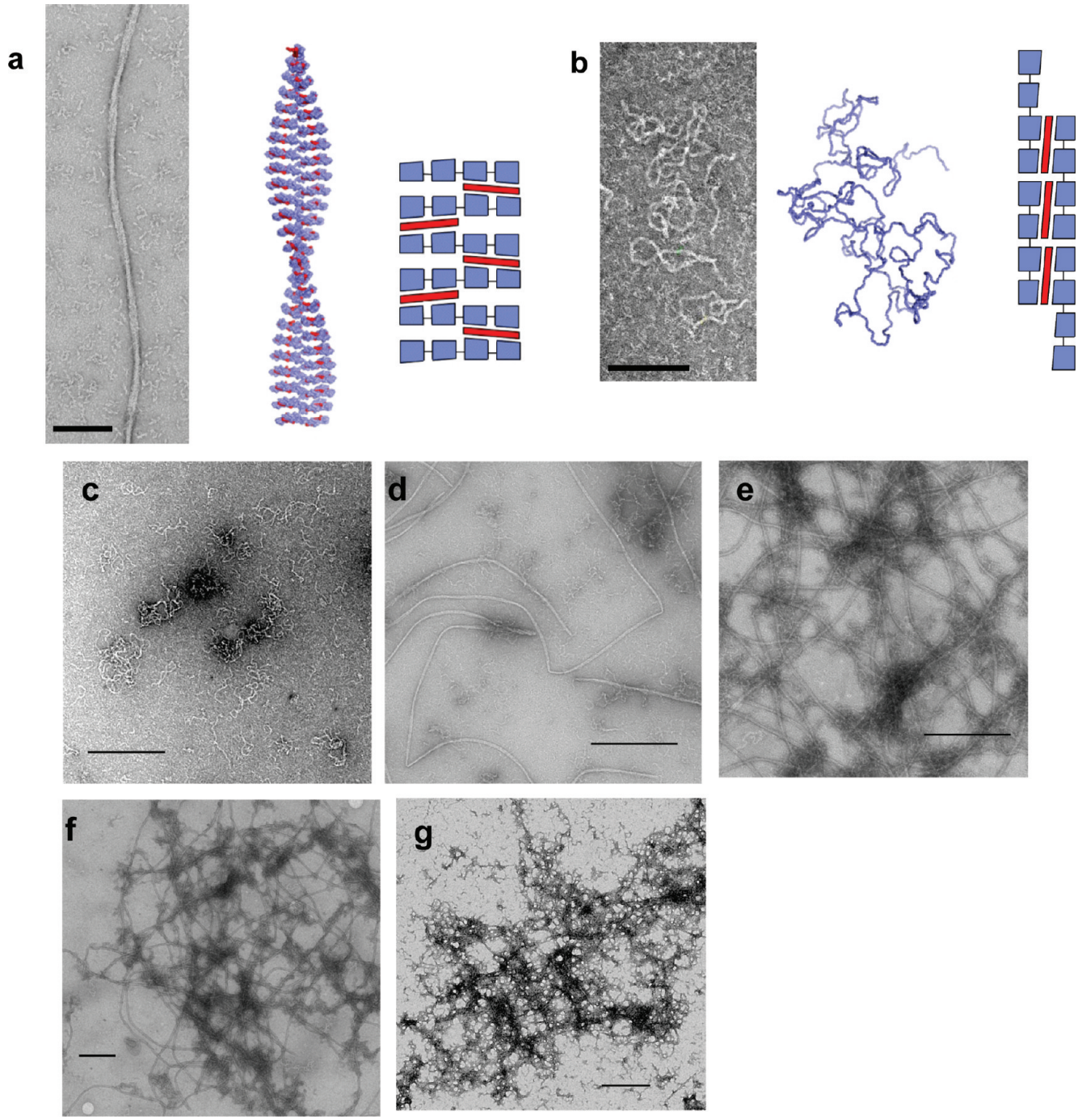

FIGURE 2. Fiber morphologies. Tapelike, semirigid fibers exhibiting helicity (a) and curly, flexible fibrils (b). For each morphology, TEM images of negatively stained samples (left), computer models derived from assembly simulations (center), and 2D schematic representations of the arrangement of building blocks (right) are shown. Tapelike fibers are interpreted in terms of stacking interactions perpendicular to the fibril axis while curly formations are likely to derive from longitudinal arrangements. The 2D representations are qualitative (no specific orientation of protein units is implied). Color code is as in Figure 1. Scale bars correspond to 100 nm. (c–g) TEM images of assembly mixtures showing (c) curly fibers (morphology ii) and (d–g) tapelike fibers (morphology i) intergrown with the curly fibrils forming a mesoscopic network. Scale bars correspond to 500 nm. In the mesh, the tapelike fibers span long distances acting as a supporting skeleton and the curly fibers form localized clusters embedded in the interstices.

recognition motifs. We envisage that functionalized NPs can contribute to further increase or diversify the intrinsic capabilities of these nanofibers in the generation of a complex bioreactive scaffold.

Acknowledgment. This work was supported by the Swiss National Foundation (Grants 3100A0-112595 to O.M. and L.K. and 3100A0-108299 to A.E.) and by the Maurice E. Müller Foundation. D.G.F. and L.D. thank the Human Fron-

DOI: 10.1021/nl1024886 | *Nano Lett.* **XXXX,** *xxx,* 000–000

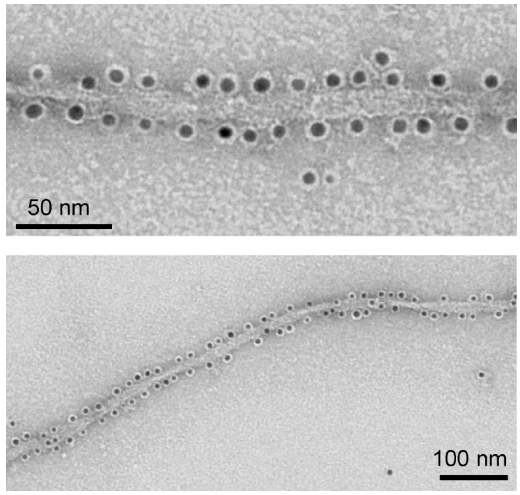

FIGURE 3. Fibers decorated with gold nanoparticles. TrisNiNTA−AuNPs are specifically attached to the hexahistidine peptides fused to the N-terminus of Tel. The specificity of the attachment is demonstrated by an extremely low background, virtually devoid of particles. AuNPs are 5.4 ± 0.6 nm in diameter and their added Mix/TrisNiNTA matrix[24] (seen as a light halo) is ~1.2 nm.

tiers Science Programme and the North West Cancer Research Fund.

Supporting Information Available. Details of production of building blocks and fiber samples, estimation of oligomeric state of engineered Z_{1212} tandems by size exclusion chromatography combined with multiangle light scattering, electron microscopy studies, and computer simulations on propagative fiber assembly modes. This material is available free of charge via the Internet at http://pubs.acs.org.

REFERENCES AND NOTES

(1) Domingo, G. J.; Orru, S.; Perham, R. N. *J. Mol. Biol.* **2001**, *305*, 259–267.
(2) Moll, D.; Huber, C.; Schlegel, B.; Pum, D.; Sleytr, U. B.; Sara, M. *Proc. Natl. Acad. Sci. U.S.A.* **2002**, *99*, 14646–14651.
(3) Padilla, J. E.; Colovos, C.; Yeates, T. O. *Proc. Natl. Acad. Sci. U.S.A.* **2001**, *98*, 2217–222.
(4) Raman, S.; Machaidze, G.; Lustig, A.; Aebi, U.; Burkhard, P. *Nanomedicine* **2006**, *2*, 95–102.
(5) Grueninger, D.; Treiber, N.; Ziegler, M. O. P.; Koetter, J. W. A.; Schulze, M.-S.; Schulz, G. E. *Science* **2008**, *319*, 206–209.
(6) Ghirlanda, G.; Lear, L. D.; Ogihara, N. L.; Eisenberg, D.; DeGrado, W. F. *J. Mol. Biol.* **2002**, *319*, 243–253.
(7) Ballister, E. R.; Lai, A. H.; Zuckerman, R. N.; Cheng, Y.; Mougous, J. D. *Proc. Natl. Acad. Sci. U.S.A.* **2008**, *105*, 3733–3738.
(8) Zhang, S. *Nat. Biotechnol.* **2003**, *21*, 1171–1178.
(9) Gras, S. L.; Tickler, A. K.; Squires, A. M.; Devlin, G. L.; Horton, M. A.; Dobson, C. M.; MacPhee, C. E. *Biomaterials* **2008**, *29*, 1553–1562.
(10) Woolfson, D. N.; Ryadnov, M. G. *Curr. Opin. Chem. Biol.* **2006**, *10*, 559–567.
(11) Baxa, U.; Speransky, V.; Steven, A. C.; Wickner, R. B. *Proc. Natl. Acad. Sci. U.S.A.* **2002**, *99*, 5253–5260.
(12) Baldwin, A. J.; Bader, R.; Christodoulou, J.; MacPhee, C. E.; Dobson, C. M.; Barker, P. D. *J. Am. Chem. Soc.* **2006**, *128*, 2162–2163.
(13) Teixeira, A. I.; Abrams, G. A.; Bertics, P. J.; Murphy, C. J.; Nealey, P. F. *J. Cell Sci.* **2003**, *116*, 1881–1192.
(14) Dalby, M. J.; Riehle, M. O.; Sutherland, D. S.; Agheli, H.; Curtis, A. S. G. *Biomaterials* **2004**, *25*, 5415–5422.
(15) Maheshwari, G.; Brown, G.; Lauffenburger, D.; Wells, A.; Griffith, L. *J. Cell Sci.* **2000**, *113*, 1677–1686.
(16) Ryadnov, M. G.; Woolfson, D. N. *J. Am. Chem. Soc.* **2004**, *126*, 7454–5.
(17) Villard, V.; Kalyuzhniy, O.; Riccio, O.; Potekhin, S.; Melnik, T. N.; Kajava, A. V.; Rüegg, C.; Corradin, G. *J. Peptide Sci.* **2006**, *12*, 206–212.
(18) Williams, A. D.; Shivaprasad, S.; Wetzel, R. *J. Mol. Biol.* **2006**, *357*, 1283–1294.
(19) Kheterpal, I.; Wetzel, R. *Acc. Chem. Res.* **2006**, *39*, 584–93.
(20) Ogihara, N. L.; Ghirlanda, G.; Bryson, J. W.; Gingery, M.; DeGrado, W. F.; Eisenberg, D. *Proc. Natl. Acad. Sci. U.S.A.* **2001**, *98*, 1404–1409.
(21) Zou, P.; Pinotsis, N.; Lange, S.; Song, Y. H.; Popov, A.; Mavridis, I.; Mayans, O.; Gautel, M.; Wilmanns, M. *Nature* **2006**, *439*, 229–233.
(22) Marino, M.; Zou, P.; Svergun, D.; Garcia, P.; Edlich, C.; Simon, B.; Wilmanns, M.; Muhle-Goll, C.; Mayans, O. *Structure* **2006**, *14*, 1437–1447.
(23) Lee, E. H.; Hsin, J.; Mayans, O.; Schulten, K. *Biophys. J.* **2007**, *93*, 1719–1735.
(24) Duchesne, L.; Gentili, D.; Comes-Franchini, M.; Fernig, D. G. *Langmuir* **2008**, *24*, 13572–1358.
(25) Kodama, H.; Matsumura, S.; Yamashita, T.; Mihara, H. *Chem. Commun.* **2004**, *24*, 2876–2877.
(26) Kasotakis, E.; Mossou, E.; Adler-Abramovich, L.; Mitchell, E. P.; Forsyth, V. T.; Gazit, E.; Mitraki, A. *Biopolymers* **2009**, *92*, 164–172.

DOI: 10.1021/nl1024886 | *Nano Lett.* **XXXX,** *xxx,* 000–000